Applied Energy 357 (2024) 122463

Contents lists available at ScienceDirect

Applied Energy

journal homepage: www.elsevier.com/locate/apenergy

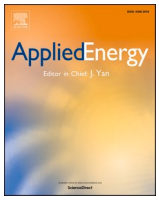

Assessing the techno-economic viability of a trigeneration system integrating ammonia-fuelled solid oxide fuel cell

Dibyendu Roy, Sumit Roy *, Andrew Smallbone, Anthony Paul Roskilly

Department of Engineering, Durham University, Durham DH1 3LE, UK

HIGHLIGHTS

- Techno-economic assessment of a trigeneration system fuelled by green ammonia.
- Trigeneration system's highest exergy efficiency is projected to be 60.94%.
- Lowest levelized cost of energy (LCOE) calculated to be £0.1232 per kWh.
- The system produces maximum power, heating, and cooling: 357.6 kW, 257.9 kW, and 46.99 kW.
- System has potential to meet UK supermarkets' energy needs while mitigating GHG emissions.

GRAPHICAL ABSTRACT

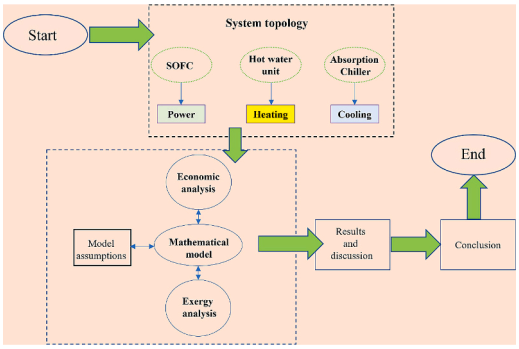

ARTICLE INFO

Keywords:
SOFC
Ammonia
Trigeneration
Techno-economic analysis
Exergy analysis
Energy system

ABSTRACT

In recent years, ammonia has gained traction as a clean fuel alternative and a promising energy carrier. In this study, a trigeneration system fuelled by ammonia has been conceptualised, integrating a solid oxide fuel cell stack for power generation, a hot water unit for heating, and an NH_3-H_2O absorption chiller for cooling. The main objective of this study is to conduct a comprehensive techno-economic feasibility assessment of the proposed trigeneration system. The system's performance was analysed for a UK supermarket requiring electricity, heating, and cooling. A detailed sensitivity analysis was performed to investigate the influence of significant operating parameters, including current density, fuel utilisation factor, and cell temperature, on the system's performance. The system can deliver maximum power, heating, and cooling outputs of 357.6 kW, 257.9 kW, and 46.99 kW, respectively. The trigeneration system is projected to achieve its highest exergy efficiency at 60.94%, with a maximum fuel energy saving ratio of 47.67%. The lowest levelised cost of energy (LCOE) is estimated to be £0.1232 per kWh. This study's objective is also aligned with United Nations Sustainable Development Goal (SDG) No. 7, which aims to achieve "Affordable and Clean Energy".

1. Introduction

The United Kingdom's net zero strategy sets an ambitious target to

* Corresponding author.
E-mail addresses: dibyendu.roy@durham.ac.uk (D. Roy), sumit.roy@durham.ac.uk (S. Roy), andrew.smallbone@durham.ac.uk (A. Smallbone), anthony.p.roskilly@durham.ac.uk (A.P. Roskilly).

https://doi.org/10.1016/j.apenergy.2023.122463
Received 21 June 2023; Received in revised form 6 November 2023; Accepted 2 December 2023
Available online 22 December 2023

Nomenclature

A_{SOFC}	Total area of solid oxide fuel cell (m^2)
CAP_i	Capital cost of i^{th} component ($)
CC	Annual capital cost (£)
CEPCI	Chemical Engineering Plant Cost Index
CRF	Capital recovery factor
$\dot{E}$	Exergy (kW)
F	Faraday's constant (C/mol)
FC	Yearly fuel cost (£)
FESR	Fuel energy saving ratio (%)
G	Gibbs energy
$\overline{h}$	Specific enthalpy (kJ/mol)
H	Annual operating hours (hr)
HEX	Heat exchanger
i_n	Interest rate (%)
i_x	Current density in x direction
$LCOE$	Levelised cost of energy (£/kWh)
LHV	Lower heating value (kJ/kg)
$\dot{m}$	Mass flowrate (kg/s)
MF	Multiplication factor
$\dot{n}$	Molar flowrate
$O\&M$	Operation and maintenance cost (£)
$\dot{Q}$	Heat transfer (kW)
R	Universal gas constant
RC	Replacement cost (£)
$\overline{s}$	Specific entropy
SFC	Specific fuel consumption
SOFC	Solid oxide fuel cell
T	Temperature
UC	Capital utilisation
V	Voltage (V)
$\dot{W}$	Power output (kW)
x_i	molar fraction of the i^{th} composition of the gas mixture
YE	Yearly expenditure (£)

Greek letters

η	Efficiency (%)

Subscripts

AB	Afterburner
AC	Air compressor
Ch	Chemical
En	Energy
EVA	Evaporator
Ex	Exergy
FC	Fuel compressor
i	Inlet
o	Outlet
Ph	Physical
0	Standard condition

power the country solely by clean electricity by 2035, subject to the security of supply [1]. Moreover, the strategy aims to install low-carbon heating appliances in all homes and workplaces by that time. To achieve this target, green hydrogen produced by splitting water molecules using electricity from renewable sources could play a significant role. However, the process of generating green hydrogen is comparatively expensive when compared to other more convenient methods of hydrogen production. Although several groups are advocating for the use of hydrogen in home heating, it is essential to note that using hydrogen for heating purposes is far less efficient than utilising electricity directly [2]. Nevertheless, the UK government plans to decide on the role of hydrogen in heating applications by 2026 [1].

In recent years, ammonia has gained traction as a clean fuel alternative and a promising energy carrier. This trend has been attributed to the growing focus on reducing carbon emissions and the need for sustainable energy sources. As reported in [3], green ammonia can serve as a carbon-free hydrogen carrier. The production of green hydrogen and nitrogen using renewable energy sources such as solar or wind energy can lead to the generation of ammonia through the Haber-Bosch principle [4]. At −33 °C temperature under ambient pressure, or at around 10 bars of pressure and atmospheric temperature ammonia can be liquefied with ease [5]. Also, compared to hydrogen, ammonia is less prone to flammability, and in case of any leakage, it can be promptly identified. It is not considered as a flammable substance at concentration less than 16% [6].

In recent years, there has been a notable surge of interest in solid oxide fuel cells (SOFCs) owing to their exceptional performance and lower environmental footprint [7]. Operating within a temperature range of 600 to 1000 °C, these fuel cells are designed to function at elevated temperatures, making them highly efficient, fuel-flexible, and capable of generating electricity with lower emissions [8]. One of the unique features of SOFCs is that they produce a by-product of high-grade waste heat that can be utilised in cogeneration or tri-generation applications. Another advantage of SOFCs is that they can be operated with a wide range of fuels, including biogas [9], syngas [10], methane, natural gas [11], methanol [12] and even ammonia [13]. These fuels can be obtained from various sources, such as renewable energy sources, and can be used to generate clean and reliable electricity. The development of SOFCs has opened up new avenues for clean energy production and has the ability to significantly decrease greenhouse gas emissions. Furthermore, SOFCs have high efficiency, fuel flexibility, and ability to produce high-quality waste heat that can be utilised in cogeneration or trigeneration applications [14]. Various studies have explored the integration of SOFCs as prime movers in cogeneration and trigeneration configurations. For instance, Al-Rashed et al. [15] investigated a cogeneration system based on an SOFC fuelled by syngas and biogas, integrated with a vanadium-chlorine cycle to generate electricity and hydrogen. The study revealed that the biogas-fuelled configuration outperformed the syngas-fuelled one, with the extent of superiority varying between 3% to 10% depending on operating conditions. Wang et al. [16] explored a trigeneration system that combined an SOFC, a gas turbine, a dual-effect absorption chiller, and solar-based energy storage to generate cooling, heating, and electricity, achieving energy and exergy efficiencies of 92.21% and 37.59%, respectively. In a separate study, Hou et al. [17] investigated a complex trigeneration system integrating a biomass-based SOFC, a double-flash binary geothermal cycle, a water heater, and a humidification-dehumidification (HDH) desalination system, achieving an optimum exergy efficiency of 64.49% and a unit cost of the product of $4.94/GJ. Similarly, Sinha et al. [18] investigated biomass-fuelled SOFC and gas turbine (GT) integrated hybrid systems employing thermodynamic analysis and reported that the maximum thermal efficiency was 63.12% with pine sawdust. Fong and Lee [19] studied the feasibility of a trigeneration configuration with an SOFC as the prime mover for two restaurant locations in Singapore and Hong Kong, which reduced primary energy consumption and carbon dioxide emissions by up to 24% and 38%, respectively. Similarly, Cao et al. [20] investigated a trigeneration system that integrated a methane-fuelled SOFC, a combined cooling and power unit, and a proton exchange membrane electrolyser for hydrogen production, achieving optimal net power generation, cooling, and hydrogen

generation. In a separate study, Choudhary and Sanjay [21] investigated the SOFC and Intercooled Gas Turbine (ICGT) integrated hybrid cycle using an energy analysis and entropy minimisation approach, which yielded an optimal efficiency of 74.13%. In another study, Kumar et al. [22] examined the integration of an SOFC-ICGT system with an organic Rankine cycle (ORC) through energy and exergy analyses, reporting an energy efficiency level of 70%. Sinha et al. [23] also conducted a study on the SOFC-ICGT integrated cycle, comparing its performance with that of the base case ICGT cycle and an intercooled recuperated GT cycle. They reported that the SOFC-ICGT system achieved the maximum efficiency of 64.78%.

In another study, Singh et al. [24] explored a combined cooling, heating, and power (CCHP) system that integrated a reversible SOFC, an organic Rankine cycle, a metal hydride hydrogen storage system, and an absorption chiller, achieving the highest overall efficiency of 88.82% in the electrolyser mode. Moreover, Xu et al. [25] examined a CCHP system that integrated a natural gas-fuelled SOFC, an absorption chiller, and a water heater system, achieving an overall efficiency of over 80%. In a different study, Zhang et al. [26] investigated municipal waste-based plasma gasification integrated with a CCHP system with SOFC as prime mover. They reported that the system was able to reach 87.6% energy efficiency, 50% electrical efficiency and 47% exergy efficiency. Mehrpooya et al. [27] investigated a technical performance investigation of a CCHP system fuelled by natural gas for a building application with SOFC as a prime mover. They reported that the system was able to achieve 45% electrical efficiency, cooling efficiency of 58% cooling efficiency and 60% heating efficiency. Zhao et al. [28] explored a cogeneration system using thermodynamic and economic analyses integrating a biomass gasification facility, SOFC and LNG coupled CO_2 recovery unit. They reported 60.28% thermal efficiency, 66.20% electrical efficiency and 55.59% exergy efficiency of the cogeneration system. Peng et al. [29] investigated natural gas fuelled CCHP system integrating solar collector, SOFC and absorption chiller using thermodynamic analysis. The reported values for the CCHP system's exergy and electrical efficiency were 70.8% and 36.03%, respectively. In another study Akikur et al. [30] investigated economic feasibility assessment of a cogeneration system integrating reversible SOFC, PTSC and PV components in context of Malaysia. The minimum LCOE of the system was reported to be 0.045$/kWh.

There are many studies on electricity production with ammonia fuelled SOFC are found in the literature. For example, Cinti et al. [31] experimentally and numerically examined use of diluted ammonia in an SOFC stack and reported efficiency with diluted ammonia up to 50%. Al-Hamed and Dincer [32] investigated thermodynamic analysis of an ammonia fuelled SOFC based hybrid system and reported the overall energy and exergy efficiency of 61.2% and 66.3%, respectively. Selvam et al. [33] investigated thermodynamic feasibility study in SOFC system with ammonia as fuel and reported the system was able to achieve 75% energy efficiency. In a recent study by a group of researchers from China [34] investigated part load performance investigations of an SOFC based system fuelled by ammonia and integrated with hydrogen regeneration sub-system and reported the overall system efficiency of 60%.

Upon reviewing the existing literature, it becomes apparent that there is a noticeable gap in research pertaining to trigeneration systems powered by SOFCs utilising ammonia as a fuel source. Comprehensive techno-economic investigations focused on ammonia-based SOFC applications are notably scarce. In light of this, our study seeks to address this gap by exploring a trigeneration system that seamlessly integrates SOFC technology, NH_3-H_2O based absorption chiller, and a water heater. This system is tailored for application in UK supermarkets, where the simultaneous demand for electricity, heating, and cooling is prevalent. Green ammonia has been chosen as a fuel for the SOFC, and a detailed techno-economic performance analysis has been performed. Furthermore, this study aligns with the objectives of United Nations Sustainable Development Goal (SDG) No. 7, which strives to achieve "Affordable and Clean Energy" [35] by offering a sustainable and efficient solution for energy generation, promoting access to affordable and clean energy, and reducing environmental impacts. With the aim of achieving the SDG No.7 this study offers a comprehensive examination of the technical and economic facets of an energy hub centred around SOFC technology, meeting the electricity, heating, and cooling needs of supermarkets in the United Kingdom. The major contributions of this study are listed below:

- A novel trigeneration system that employs green ammonia as a fuel source has been introduced. This system integrates an SOFC stack for power generation, a hot water generation unit for heating, and an NH_3-H_2O absorption chiller for cooling. It is specifically tailored for the unique energy demands of supermarkets in the UK.
- Comprehensive analyses of technical and economic feasibility for the trigeneration system have been presented.
- Sensitivity analysis has been performed on various technical and economic parameters.
- The results of the proposed trigeneration system have been compared with various types of trigeneration systems.

The organisation of the paper is summarised in Fig. 1. Firstly, in the "materials and methods" section, the system configuration has been introduced. Secondly, numerical model of SOFC is explained and verified with experimental results. Thirdly, exergy and economic models are explained. Furthermore, in "Results and discussion" section, the sensitivity analysis of important technical and economic parameters are performed. Additionally, the proposed trigeneration system have been compared with previous trigeneration systems reported in the literature. Finally, the conclusions are summarised.

2. Materials and methods

2.1. System topology

A schematic representation of the ammonia-fuelled SOFC-based trigeneration system is presented in Fig. 2. The integrated system comprises an SOFC stack for power generation, a hot water generation unit for heating, and an NH_3-H_2O absorption chiller for cooling. Ammonia fuel is stored at −33 °C and is preheated in heat exchangers HEX1 and HEX3 before being fed into the anode channel of the SOFC. Similarly, hot air is directed into the cathode channel after being heated by HEX4. Any unutilised fuel exiting the anode channel of the SOFC unit is completely combusted in the afterburner unit. The exhaust gas from the afterburner unit is divided into two streams using a splitter. One stream is used to preheat the incoming cathode channel air at HEX4, and the other stream is used to preheat the incoming fuel for the anode channel at HEX3. Additionally, these two streams are mixed and employed to heat the incoming fresh water supplied by a water pump at the HEX2 heat exchanger unit. Furthermore, the hot water is used to provide heat to the generator of the absorption chiller. The NH_3-H_2O absorption chiller consists of several subunits: Generator, Condenser, Refrigerant HEX, Evaporator, Absorber, Solution Pump, and Solution HEX. In this absorption chiller, ammonia serves as the refrigerant, and water acts as the absorbent. Under reduced pressure, the refrigerant undergoes vaporization within the evaporator and is then absorbed into the weak ammonia-water solution within the absorber.

The modelling of the system is based on the following technical input parameters provided in Table 1. To simplify the analysis, the following assumptions have been made [36]:

- The trigeneration system functions while operating at a steady state and under thermodynamic equilibrium conditions.
- The gases behave as an ideal gas.
- SOFC is completely insulated and no heat loss from the SOFC has been considered.

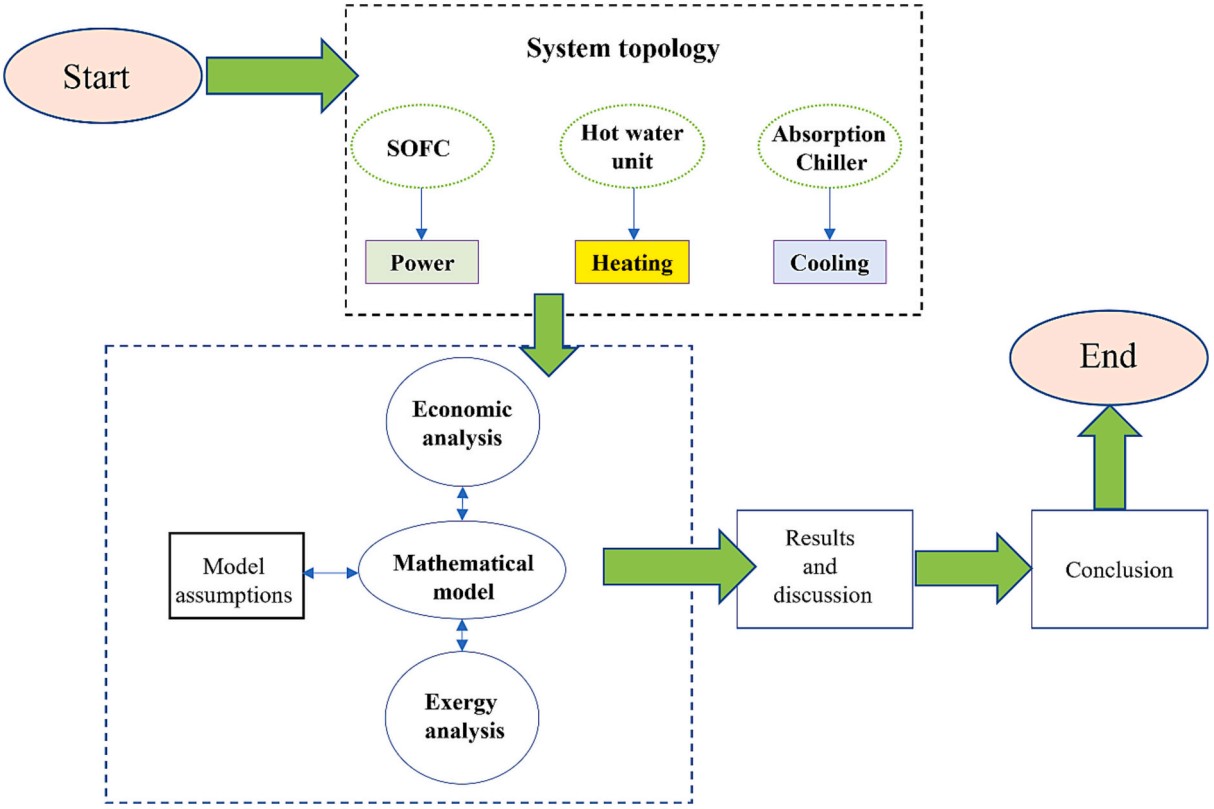

Fig. 1. Analysis procedure and organisation of the study.

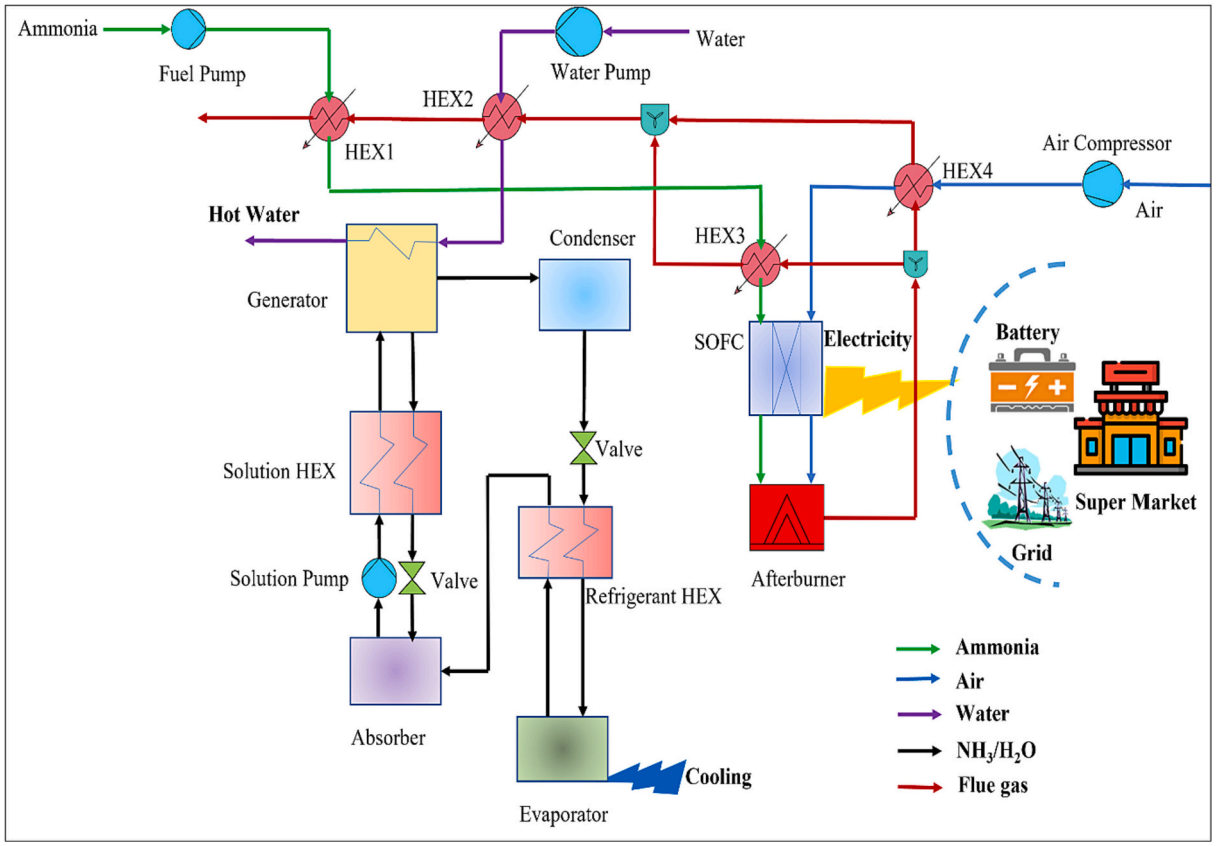

Fig. 2. Proposed ammonia fuelled SOFC based trigeneration system.

Table 1
Technical specifications.

Description	Value	Unit	Ref.
Operating cell temperature of SOFC	650–900	°C	[37]
Operating current density of SOFC	2000–5000	A/m^2	[38]
Fuel utilisation factor	0.7–0.9	–	[37]
Pressure difference anode	0.02	bar	[39]
Pressure difference cathode	0.02	bar	[39]
DC-AC conversion efficiency	96	%	[39]
Pressure loss in heat exchangers	0.01	bar	[39]
Compressor isentropic efficiency	70	%	[39]
Compressor mechanical efficiency	80	%	[39]
Isentropic efficiency of pump	85	%	[39]
Mechanical efficiency of pump	60	%	[39]
Ammonia storage temperature	−33	°C	[39]
Domestic hot water temperature	65	°C	–
Evaporator temperature	−5	°C	[40]
Reflux ratio	0.13	–	[41]
Solution pump isentropic efficiency	65	%	[41]
η_{REF}	40	%	[42]
η_{boiler}	90	%	[42]

- Temperatures at the inlet channels of SOFC are identical, similarly the temperatures at the exit channels of SOFC are same.
- All the unreacted fuels coming from the SOFC module are completely burned at the afterburner.

It should be noted that the described system has been modelled in a manner that ensures its optimal operation and efficiency. The system's technical input parameters have been carefully selected and are based on available literature and industry standards. The assumption of steady-state operation ensures that the system operates at a consistent level, which allows for accurate analysis of the system's performance over time.

The schematic representation of the ammonia fuelled SOFC based trigeneration system presented in Fig. 2 is designed to provide a clear and detailed understanding of the system's operation. The system's various components have been clearly identified, and their functions have been explained in detail. Additionally, the technical input parameters provided in Table 1 have been selected to ensure that the system is modelled accurately, taking into account all the relevant parameters required for optimal system operation.

The described methodology is a comprehensive and detailed representation of the ammonia fuelled SOFC based trigeneration system. The methodology is designed to provide a clear and accurate understanding of the system's operation and efficiency, and the assumptions made in the analysis ensure that the results are reliable and relevant.

2.2. Solid oxide fuel cell

The reversible voltage, also known as the Nernst voltage, of the SOFC can be calculated using the following equation[33].

$$V_x = V_T^0 + \frac{\mathrm{R}T_{cell}}{2\mathrm{F}} ln\left\{\frac{x_{O_2,ca}^{1/2} \times x_{H_2,an}}{x_{H_2O,an}} \times p_{cell}^{1/2}\right\} \quad (1)$$

where 'F' denotes Faraday's constant, which is equal to 96,487C per mole. 'p' denotes the partial pressure of the cell, 'R' is the universal gas constant, T_{cell} is the operating temperature of the fuel cell, and 'x' refers to the molar fraction of the relevant element present in the cathode (ca) and anode (an) streams. V_T^0 is the standard reversible voltage and it can be estimated from the change in Gibbs energy as shown below [33].

$$V_T^0 = +\frac{\Delta G_T^0}{2F} \quad (2)$$

The voltage generated by the cell is lesser than the reversible voltage due to the irreversible operations of the cell. The disparity between the reversible voltage and the actual voltage is denoted by the voltage loss, as demonstrated underneath [43]:

$$V = V_x - \Delta V_{Loss} \quad (3)$$

Similar to Ohm's law, the constant of proportionality is represented by the equivalent cell resistance (R_{eq}), which can be defined as follows.

$$R_{eq} = \frac{\Delta V_{Loss}}{i_x} \quad (4)$$

Lastly, the rate at which H_2 is converted at a given cross-section x can be determined by the current density:

$$\frac{dn_{H_2}}{dx} = \frac{i_x}{2F} \quad (5)$$

The calculation of the net electrical power generated by SOFC ($\dot{W}_{SOFC}$) is based on the following equation.

$$\dot{W}_{SOFC} = V \times I \times \eta_{DC/AC} \quad (6)$$

where $\eta_{DC/AC}$is the inverter efficiency.

The results of this SOFC model were compared with the experimental findings by Wang et al. [44] and the numerical results by Selvam et al. [33]. To assess the model's performance, ammonia was utilised as the fuel, and the cell temperature was maintained at 750 °C. Fig. 3 illustrates the current density versus cell voltage characteristics of the current model, compared to both experimental and numerical results. The comparison shows that the model exhibits a maximum difference of only 1.29% from the experimental data and 2.73% from the numerical results.

2.3. Exergy analysis

It is considered that the exergy ($\dot{E}$) value of each stream is a summation of its physical and chemical exergy [41].

$$\dot{E} = \dot{E}_{Ph} + \dot{E}_{Ch} \quad (7)$$

where $\dot{E}_{Ph}$and $\dot{E}_{Ch}$ represent physical exergy and chemical exergy, respectively. The equations, given below, can be used to estimate physical exergy and chemical exergy values.

$$\dot{E}_{Ph} = \sum_i \dot{n}_i((\overline{h}_i - \overline{h}_0) - T_0(\overline{s}_i - \overline{s}_0)) \quad (8)$$

where $\overline{h}$, $\overline{s}$ and $\dot{n}$ are the specific enthalpy, specific entropy, and molar flowrate, respectively. The subscript 0 indicates the reference state

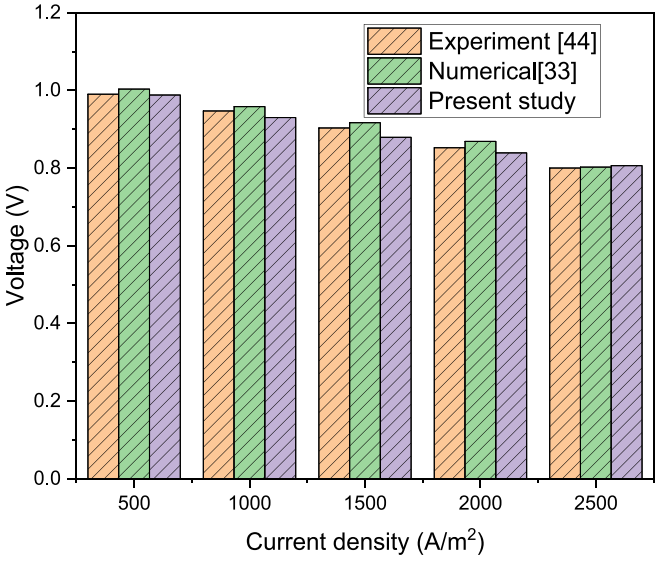

Fig. 3. SOFC model validation.

(T_0 = 25 °C and p_0 =101.325 kPa).

$$\dot{E}_{Ch} = \dot{n}\left(\sum_i x_i \overline{e}_i^{Ch,0} + \overline{R}T_0 \sum_i x_i ln(x_i)\right) \quad (9)$$

where $\overline{e}_i^{Ch,0}$ and x_i are the standard chemical exergy and molar fraction of the ith composition of the gas mixture, respectively.

2.4. Economic analysis

Table 2 shows the primary input data needed for the economic analysis.

It is considered that the SOFC stacks are replaced in every 5 years [51]. Yearly expenditure (YE) is estimated by the following relation.

$$YE = CC + O\&M + RC + FC \quad (10)$$

where, *CC:* Capital cost, O&M: operation and maintenance cost, FC: yearly fuel cost, and *RC*: replacement cost.

The estimation of the annual Capital Cost (CC) is based on the following equation

$$CC = TCC \times (1 + MF_{PC}) \times (1 + MF_{TPC}) \times (1 + MF_{TOP}) \times CRF \quad (11)$$

The estimation of total capital cost (*TC*) is based on the following equation

$$TCC = \sum_i CAP_i \quad (12)$$

The capital recovery factor (CRF) is defined by the relation provided below.

$$CRF = \frac{i_n(1+i_n)^{yr}}{(1+i_n)^{yr} - 1} \quad (13)$$

where, $i_n$and *yr* are "annual interest rate" and "operational years", respectively.

Table 3 provides the cost functions of various components. Chemical Engineering Plant Cost Index (CEPCI) was used to update the equipment cost functions. The equipment cost of its ith component was updated using the equation below [52].

$$CAP_{i,2022} = CAP_i \times \frac{CEPCI_{2022}}{CEPCI_{OY}} \quad (14)$$

where, respectively, the cost indices *CEPCI 2022* and *CEPCI OY* stand for the year 2022 and the original year the cost relation was established.

2.5. Performance indicators

The overall energy efficiency of the system is estimated by the following equation:

$$\eta_{En} = \frac{\dot{W}_{net} + \dot{Q}_{heating} + \dot{Q}_{cooling}}{\dot{m}_{fuel} \times LHV_{fuel}} \quad (15)$$

The electrical efficiency of the system is estimated as

$$\eta_{EL} = \frac{\dot{W}_{net}}{\dot{m}_{fuel} \times LHV_{fuel}} \quad (16)$$

The system's exergy efficiency is estimated as

$$\eta_{Ex} = \frac{\dot{W}_{net} + \dot{E}_{heating} + \dot{E}_{cooling}}{\dot{m}_{fuel} \times LHV_{fuel}} \quad (17)$$

Fuel energy saving ratio (FESR) has been estimated as follows [57].

$$FESR = \frac{FCON_{Reference\ system} - FCON_{Present\ system}}{FCON_{Reference\ system}} \quad (18)$$

$$FCON_{Reference\ system} = \frac{\dot{W}_{net}}{\eta_{REF}} + \frac{\dot{Q}_{heating}}{\eta_{boiler}} + \frac{\dot{Q}_{cooling}}{\eta_{boiler} \times COP_{VAR}} \quad (19)$$

$$FCON_{Present\ system} = \dot{m}_{fuel} \times LHV_{fuel} \quad (20)$$

The levelised cost of energy was calculated using the equation shown below [58].

$$LCOE = \frac{YE}{UC_{CAP} \times H \times (\dot{W}_{net} + \dot{Q}_{heating} + \dot{Q}_{cooling})} \quad (21)$$

where H is for annual operating hours, UC_{CAP} stands for capital utilisation parameter, and YE stands for annual plant expense.

The specific fuel consumption of the system is estimated by the equations provided below

$$SFC = \frac{3600 \times \dot{m}_{fuel}}{(\dot{W}_{net} + \dot{Q}_{heating} + \dot{Q}_{cooling})} \quad (22)$$

Table 2
Input parameters for economic analysis.

Description	Value	Unit	Ref.
Operational year	30	years	[45]
Number of operating hours per year	8000	hr	[46]
UC_{CAP}	85	%	[47]
Cost of ammonia	0.57	£/kg	[48]
i_n	3	%	[49]
MF_{TOP}	20.20	%	[50]
MF_{TPC}	52.5	%	[50]
MF_{PC}	9	%	[50]

3. Results and discussion

3.1. Effect of current density on the performance of the system

The results of the current density on the performance of the ammonia-fuelled SOFC-based trigeneration system are presented in this section. The graphical representation of the system performance with respect to operating current density is presented in Fig. 4. The impact of operating current density on net power output, heating, and cooling production is illustrated in the figure. It is evident from the figure that increasing the current density results in a corresponding increase in the net power output, heating, and cooling production. The reason behind this phenomenon is that at higher current densities, a greater amount of fuel is consumed, leading to the generation of more power. The highest net power output of 357.6 kW was obtained at a current density of 5000 A/m^2. Moreover, as the flue gas mass flow rate increases from the exit of the SOFC module at higher operating current densities, more waste heat is generated, resulting in higher heating and cooling production. The current density of 5000 A/m^2 resulted in the maximum heating and cooling outputs of 208.5 kW and 37.98 kW, respectively. The results show that the ammonia-fuelled SOFC-based trigeneration system operates efficiently at high current densities, which is advantageous for commercial applications. The findings of this study suggest that the system can be optimised to operate at higher current densities to achieve better system performance.

The impact of operating current density on the performance of the proposed system was further investigated by analysing its energy efficiency, exergy efficiency, and fuel energy saving ratio (FESR). Fig. 5 illustrates the variation in these parameters with respect to different current densities. The results indicate that the increase in current density leads to a decline in both energy and exergy efficiency of the system, primarily due to voltage loss. The highest energy efficiency and exergy efficiency of the system were observed at a current density of 2000 A/m^2, with values of 94.32% and 60.94%, respectively. A similar trend was

Table 3
Equations for estimating capital costs of different components.

Component	Cost function	CEPCI (Ref Year)	Ref
SOFC	$C_{SOFC} = A_{SOFC}(2.96T_{SOFC} - 1907)$	395.6 (2002)	[53]
SOFC Inverter	$CAP_{inverter} = 10^5\left(\frac{\dot{W}_{SOFC.DC}}{500}\right)^{0.7}$	395.6 (2002)	[53]
Afterburner	$CAP_{AB} = \frac{46.08 \times \dot{m}_{oxydant}}{0.995 - \frac{P_{out}}{P_{in}}}[1 + exp(0.018 \times T_{out} - 26.4)]$	368.1(1994)	[53]
Air compressor	$CAP_{AC} = 1516.5 \times \left(\dot{W}_{AC}\right)^{0.67}$	402.3 (2003)	[54]
Fuel compressor	$CAP_{FC} = 1516.5 \times \left(\dot{W}_{FC}\right)^{0.67}$	402.3 (2003)	[54]
Heat exchanger	$CAP_{HEX} = 3 \times 130 \times (Area/0.093)^{0.78}$	468.2 (2005)	[53]
Chiller	$CAP_{Chiller} = 1144.3 \times \dot{Q}_{EVA}$	394.1 (2000)	[55]
Pump	$CAP_{Pump} = 3 \times 422 \times 1.41 \times \left(\frac{\dot{W}_{Pump}}{1}\right)^{0.71} \times fn$ $fn = 1 + (0.2/(1-\eta))$	394.1 (2000)	[56]

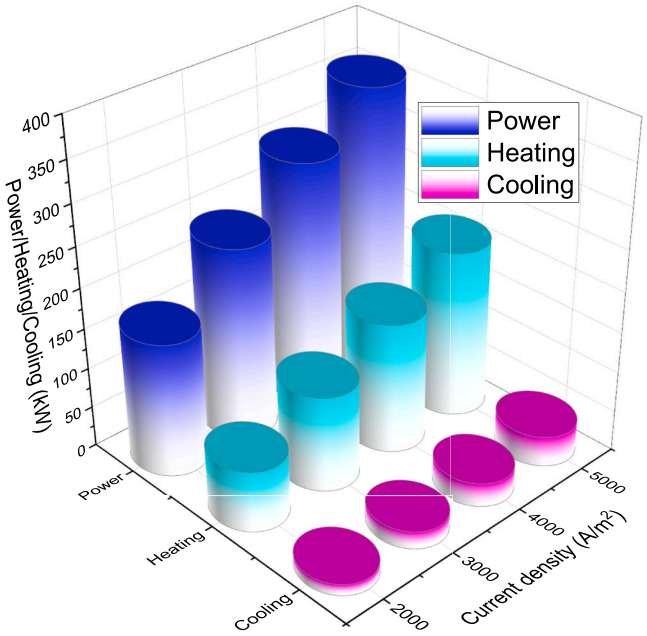

Fig. 4. Effect of current density on the power, heating, and cooling.

observed for the FESR, with the highest value of 47.67% obtained at the same current density of 2000 A/m^2. This can be attributed to the fact that the fuel consumption of the system decreases in comparison to the standard reference system at lower operating densities, leading to an increase in FESR values. It is worth noting that the energy efficiency, exergy efficiency, and FESR of the system are critical parameters that determine the overall performance of the proposed system. Therefore, it is crucial to identify the optimum operating conditions to ensure the efficient functioning of the integrated configuration. The results obtained from this study offer valuable insights into the effect of operating current density on the system's efficiency, thereby facilitating the development of more efficient and sustainable energy systems.

The results of the influence of operating current density on the performance of the SOFC system are further elaborated by examining the LCOE and specific fuel consumption. The relationship between these two parameters and the operating current density is depicted in Fig. 6. The results show that as the operating current density increases, the LCOE of the system decreases gradually. This trend is attributed to the fact that higher current densities correspond to greater values of net power output, heating, and cooling production, as shown in Fig. 4. Consequently, according to Eq. 21, LCOE decreases due to the increase in the overall energy output of the system. However, it is observed that an increase in current density leads to a higher specific fuel consumption. This is due to the increase in fuel consumption within the system at higher operating current densities. This increase in fuel consumption is due to the higher demand for fuel to meet the increased power output and waste heat recovery needs. The observed increase in specific fuel consumption with increasing current density suggests that there is a trade-off between fuel supply and system efficiency. Therefore, to optimise the performance of the SOFC system, the operating current density needs to be carefully balanced with the fuel utilisation. The results of this study provide valuable insights into the impact of operating current density on the performance of an SOFC system.

3.2. *Effect of fuel utilisation factor on the performance of the system*

The impact of fuel utilisation factor (UF) on the system's performance was investigated while holding current density and cell temperature constant. Fig. 7 illustrates the effect of UF on power, heating, and cooling outputs within the range of 0.7–0.9. The results showed that as UF levels increased, the power output, as well as the heating and cooling outputs, decreased. This decreasing trend can be attributed to the lower molar flow rate of fuel to the SOFC, which leads to a decrease in cell voltage and subsequently, a decrease in power output. At higher UF values, less waste heat is available for recovery in the heating and cooling circuit, resulting in reduced heating and cooling outputs. This is because a larger fraction of the fuel energy is consumed in the SOFC to produce electricity, leaving less energy available for heating and cooling. Therefore, there is a trade-off between the electrical and thermal energy outputs of the system, and the optimal UF value must be selected based on the specific requirements of the application. The results indicate that the net power output decreases from 308.6 kW to 295.6 kW when the UF increases from 0.7 to 0.9. Similarly, the heating and cooling outputs decrease from 257.9 kW and 46.99 kW to 89.52 kW and 16.31 kW, respectively, when the UF increases from 0.7 to 0.9.

In addition to the aforementioned results, it is worth noting that the fuel utilisation factor (UF) plays a crucial role in determining the efficiency and performance of the proposed trigeneration system. Fig. 8 provides a detailed insight into the impact of UF on the energy efficiency, exergy efficiency, and fuel energy saving ratio of the system. As the UF values increase, the energy efficiency and fuel energy saving ratio of the system decrease, indicating that more fuel is needed to generate the equal amount of electricity, heating, and cooling. The maximum

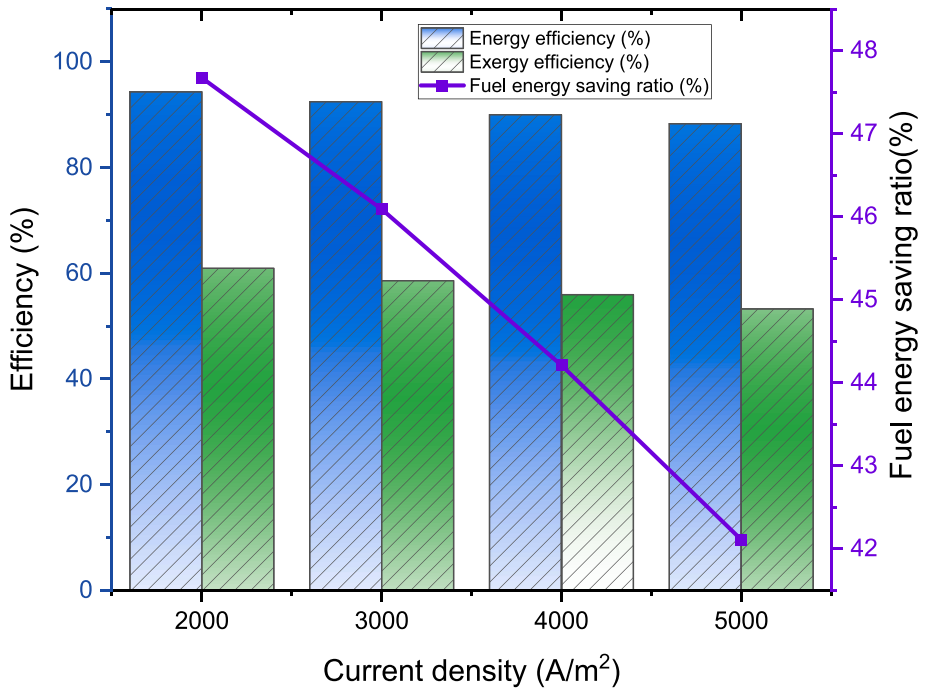

Fig. 5. Effect of current density on energy efficiency, exergy efficiency and fuel energy saving ratio of the system.

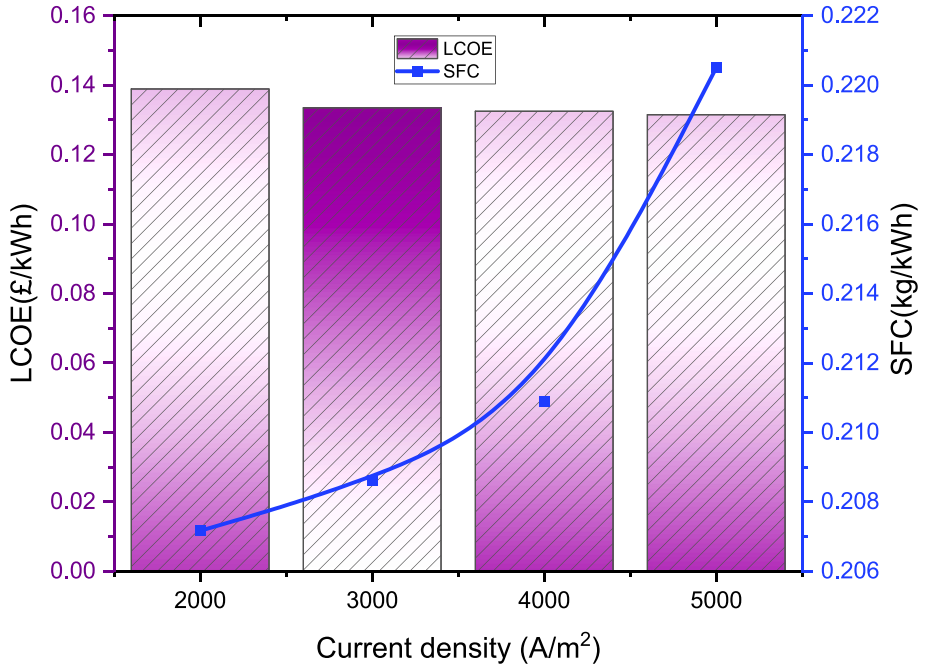

Fig. 6. Effect of current density on LCOE and specific fuel consumption of the system.

energy efficiency and fuel energy saving ratio of the system were found to be 98.07% and 44.52%, respectively, at a UF value of 0.70. On the other hand, the exergy efficiency of the system increases with an increase in UF and reaches its peak value of 59.58% at a UF value of 0.90. This behaviour can be attributed to the fact that a higher UF leads to a lower exhaust gas temperature and higher exhaust gas quality, resulting in a higher exergy efficiency. The results indicate that a UF value of 0.70 can provide the optimal balance between energy efficiency and fuel energy saving ratio, while a UF value of 0.90 can lead to the highest exergy efficiency. These outcomes can assist in the design and optimisation of similar SOFC-based trigeneration systems in the future.

In addition to the aforementioned observations, it is important to note that the levelised cost of electricity is a critical metric for evaluating the financial feasibility of energy systems. As shown in Fig. 9, the LCOE increases from 0.1232 £/kWh to 0.1491 £/kWh as the UF increases from 0.7 to 0.9, respectively. This indicates that a higher UF value leads to a higher cost of electricity production, which could negatively impact the economic viability of the SOFC system. Moreover, the increase in SFC with higher UF values signifies that more fuel is required to produce the same amount of electricity, heating, and cooling outputs. This could result in increased operating costs and reduced overall efficiency of the system. Therefore, the choice of UF value for an SOFC system should be

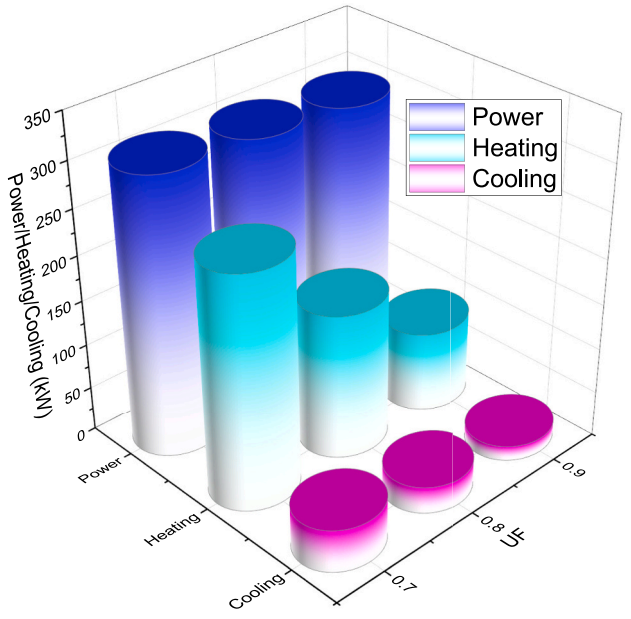

Fig. 7. Effect of fuel utilisation factor on the power, heating, and cooling.

based on a trade-off between the system's performance, efficiency, and cost-effectiveness. The results suggest that a UF value of 0.70 is the optimal value for achieving the highest energy efficiency and fuel energy saving ratio while maintaining a relatively low LCOE and SFC. However, the decision on the UF value should also consider other factors such as the availability and cost of ammonia fuel, maintenance costs, and system lifetime.

3.3. *Effect of cell temperature on the performance of the system*

In this study, the effect of cell temperature on the performance of the SOFC system was investigated. As shown in Fig. 10, the power output of the system remains relatively constant within the temperature range of 700–900 °C, while holding current density and fuel utilisation factor constant. The maximum power output of 305.2 kW was achieved at a cell temperature of 700 °C. It is observed that the heating and cooling outputs exhibit a slight increasing trend as the cell temperature is increased. This can be attributed to the increase in the operating temperature of the SOFC, which results in a slightly higher availability of waste heat from the SOFC module. It is worth noting that the effect of cell temperature on the performance of an SOFC system is complex, and can be affected by several factors, including the electrode kinetics, transport phenomena, and electrochemical performance of the system. Therefore, further investigation is needed to fully understand the impact of cell temperature on the performance of the SOFC system.

Fig. 11 illustrates the effect of cell temperature on the energy efficiency, exergy efficiency, and fuel energy saving ratio (FESR) of the system, within the range of 700–900 °C, while holding current density and fuel utilisation factor constant. It can be observed that the trends of energy and exergy efficiency of the system with rising cell temperature remain mainly constant. The maximum energy and exergy efficiency is found to be 90.61% and 56.37%, respectively, at a cell temperature of 700 °C. However, with rising cell temperature, the FESR levels tend to decrease. This is mainly due to a marginal drop in power output production, and according to Eq. 19, the fuel consumption in the reference system slightly decreases. The maximum FESR of the system is estimated to be 44.47%. Overall, the results suggest that the SOFC system is relatively insensitive to changes in cell temperature within the range studied.

Fig. 12 illustrates the impact of operating cell temperature, within the range of 700–900 °C, while holding current density and fuel utilisation factor constant, on the levelised cost of energy (LCOE) and specific fuel consumption (SFC) of the system. As shown in the figure, it is observed that the LCOE gradually increases with rising cell temperature. This is mainly due to the decrease in power output production at higher operating cell temperature, as depicted in Fig. 10. The lowest LCOE value of 0.1313 £/kWh is found at a cell temperature of 700 °C. Furthermore, it is found that the specific fuel consumption (SFC) of the system increases with increasing cell temperature. This is mainly due to the decrease in power output production with increasing cell temperature, as shown in Fig. 10. The lowest SFC value of 0.2104 kg/kWh is

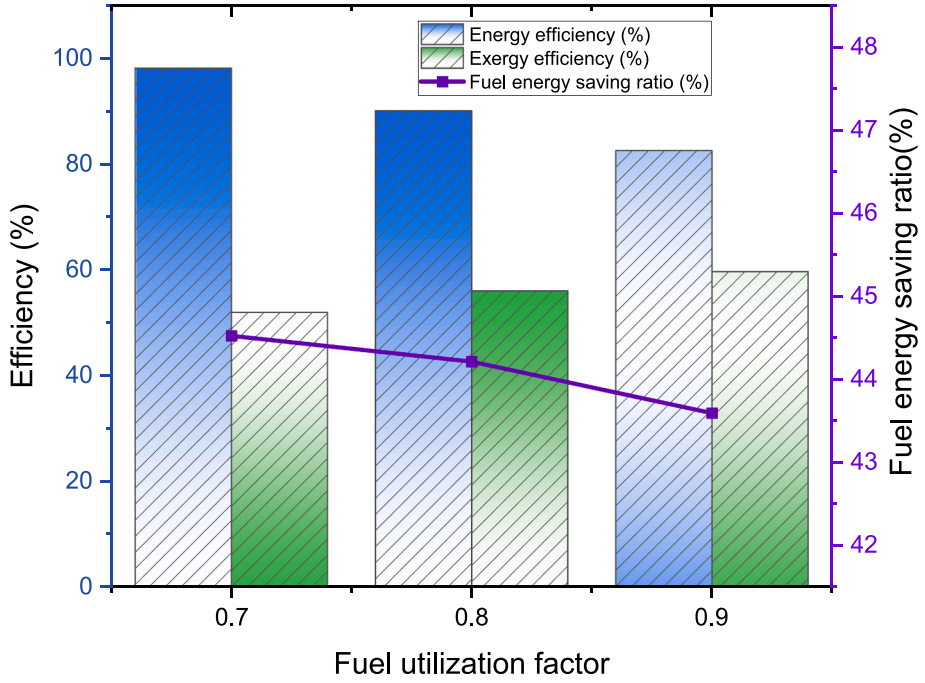

Fig. 8. Effect of fuel utilisation factor on energy efficiency, exergy efficiency and fuel energy saving ratio of the system.

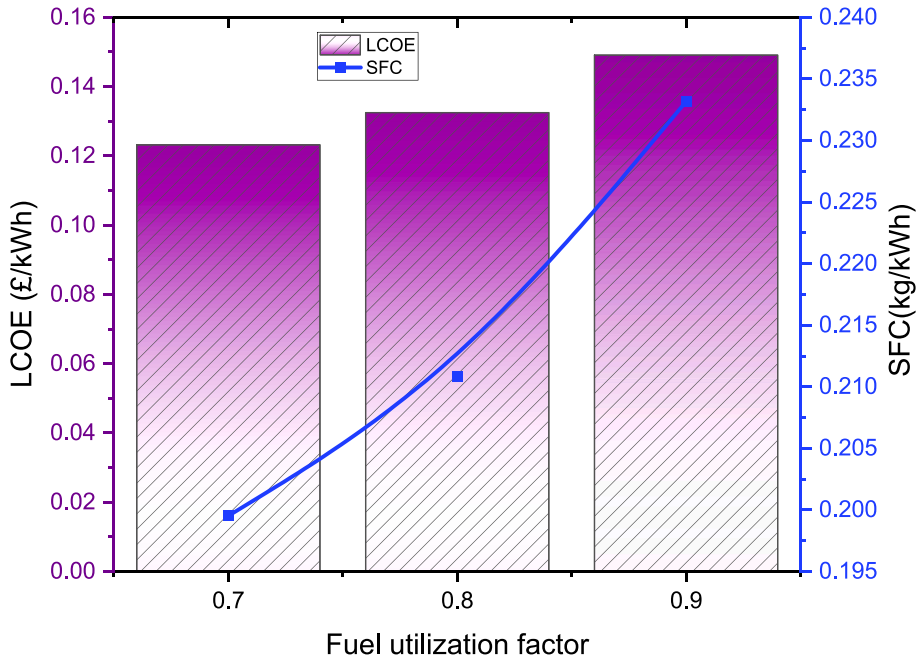

Fig. 9. Effect of fuel utilisation factor on LCOE and specific fuel consumption of the system.

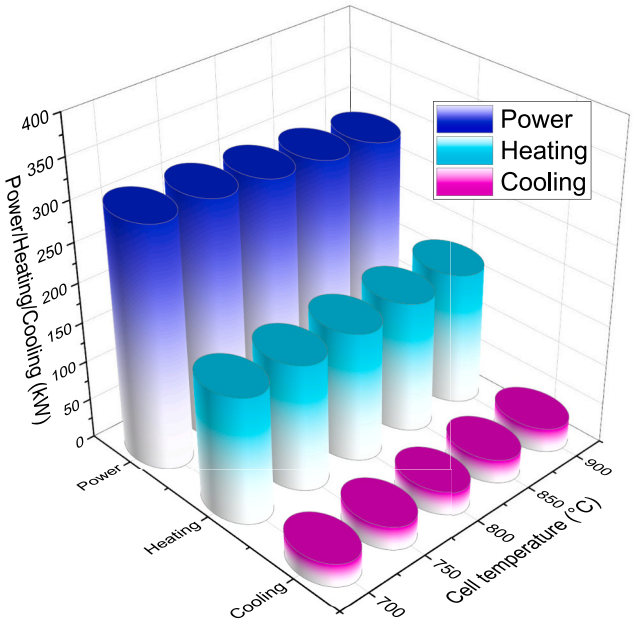

Fig. 10. Effect of cell temperature on the power, heating, and cooling.

found at a cell temperature of 700 °C. Overall, the results suggest that operating the SOFC system at a lower cell temperature, such as 700 °C, can result in lower LCOE and SFC values, indicating improved economic and environmental performance of the system.

3.4. Comparison with other systems

The results of the proposed trigeneration system have been compared with various types of trigeneration systems, and the findings are presented in Table 4. The proposed system demonstrated comparable exergy efficiency to other systems, and even outperformed some of the trigeneration systems reported in the literature. However, when considering the LCOE, other systems performed better.

3.5. Sensitivity analysis of levelised cost of energy

It is essential to note that the Levelised Cost of Energy (LCOE) analysis is highly dependent on the assumptions made regarding the system's interest rates, operating years of the proposed system and other economic parameters. Therefore, a sensitivity analysis of these assumptions is crucial to determine the most cost-effective system design and operation. This sub-section presents a sensitivity analysis of LCOE on variable interest rates and operating years. Fig. 13 illustrates the impact of interest rates on the LCOE of the system. The results show that as the interest rates increase, the LCOE values also increase. At an interest rate of 15%, the LCOE value can reach up to 0.157£/kWh, whereas at 3%, the LCOE will be 0.1325£/kWh. In addition to interest rates, the operating years of the system also significantly impact the LCOE values. Fig. 14 presents the effect of changing operating years on the LCOE values. The minimum LCOE value can be achieved at 50 years of operating years, which is 0.1296 £/kWh.

4. Conclusion

In conclusion, this article has presented a comprehensive techno-economic evaluation of a trigeneration system integrated with a solid oxide fuel cell fuelled by green ammonia, complemented by an NH_3-H_2O absorption chiller and a water heater, and its capability to deliver electricity, heating, and cooling to a UK supermarket. This research examined how several operating parameters, including current density, fuel utilisation factor, and cell temperature, impacted the system's performance. The major findings are summarised as listed below:

- The results showed that the increase in current density led to higher net power, heating, and cooling production, but lower energy and exergy efficiency.
- The levelised cost of energy decreased as the operating current density increased, but a higher specific fuel consumption was observed with higher current densities. The fuel utilisation factor and cell temperature were also found to affect the system's performance.
- The system can generate maximum power, heating, and cooling outputs of 357.6 kW, 257.9 kW, and 46.99 kW, respectively.

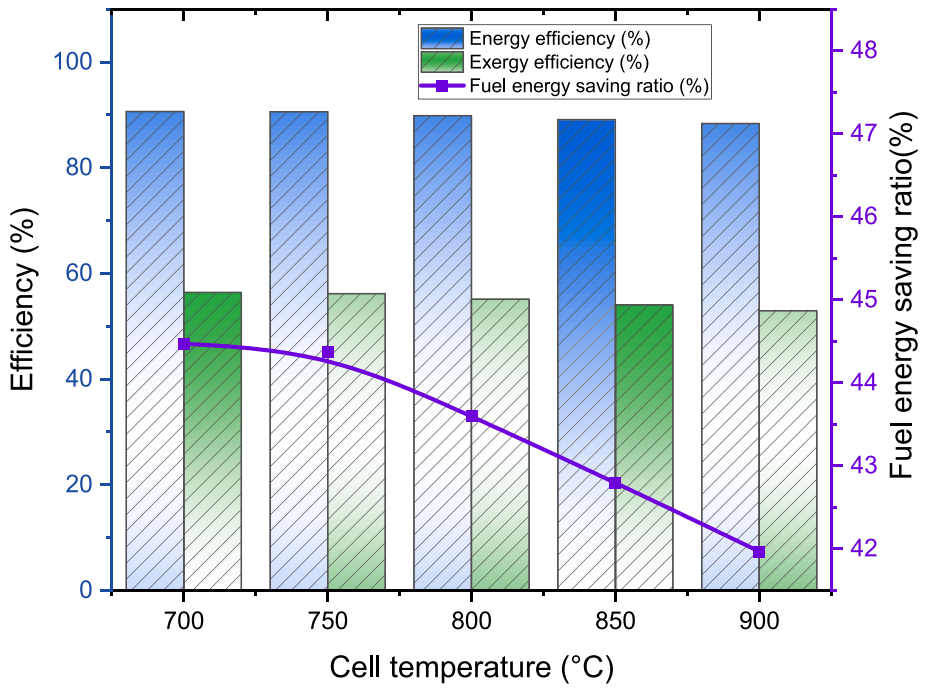

Fig. 11. Effect of cell temperature on energy efficiency, exergy efficiency and fuel energy saving ratio of the system.

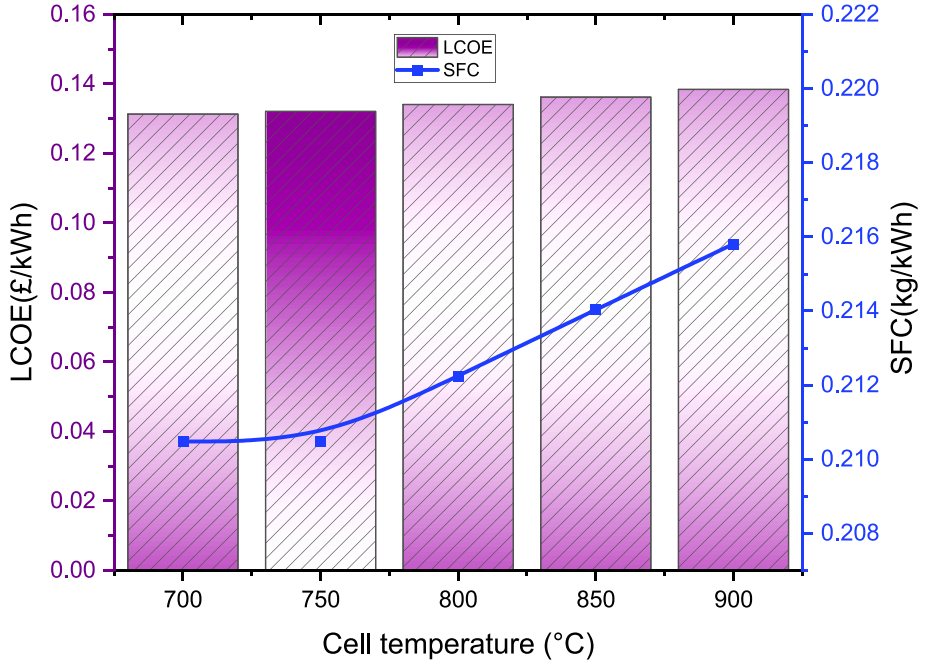

Fig. 12. Effect of cell temperature on LCOE and specific fuel consumption of the system.

- The trigeneration system's highest exergy efficiency is projected to be 60.94%, with a maximum overall energy efficiency of 98.07% and maximum fuel energy saving ratio of 47.67%.
- Sensitivity analysis revealed that the minimum LCOE value can be achieved up to 0.1232 £/kWh.

Notably, since the system employs green ammonia as fuel, there are no CO_2 emissions from the system. The study demonstrates that the proposed trigeneration system has the potential to meet the energy requirements of UK supermarkets while mitigating greenhouse gas emissions. This research provides valuable insights into designing and optimising a trigeneration system with SOFC fuelled by green ammonia for UK supermarkets. Furthermore, the future perspective of this work can expand to investigate the system in more detail, employing exergoeconomic and life cycle assessments. Additionally, it will be interesting to assess the techno-economic performance of the trigeneration system using an anode and cathode recirculation loop.

Currently, SOFC stack costs remain relatively high, necessitating cost reduction through technological advancements and large-scale commercial production. Also, extensive investigation remains imperative to address issues related to its durability and stability as SOFCs are susceptible to degradation over time due to factors like thermal stress,

Table 4
Comparative performance with trigeneration systems.

System	Energy source	Products	Efficiency	LCOE	Ref
Proton conducting SOFC and LiBr absorption chiller based trigeneration system	Hydrogen	Power, Heating and Cooling	79.31% (energy) 56.06% (exergy)	–	[59]
SOFC integrated with steam Rankine cycle, ejector refrigeration cycle, a thermoelectric generator, and an electrolyser.	Methane	Power, Cooling and Hydrogen	68.2% (energy) 58.02% (exergy)	–	[20]
SOFC based system integrated with NH_3-H_2O chiller and water heating facility	Biomass	Power, Heating and Cooling	55.99% (exergy)	0.079 $/kWh	[41]
Organic Rankine cycle integrated with single stage absorption heat transformer and single stage evaporation	Geothermal energy	Power, Hot water, and fresh water	30.47% (energy) 41.72% (exergy)	0.04026 $/kWh	[58]
Gasifier integrated with gas engine and an Absorption chiller	Biomass and natural gas	Power, Heating and Cooling	66% (energy)	0.15 $/kWh	[60]
SOFC integrated with NH_3-H_2O chiller and a hot water production facility	Ammonia	Power, Heating and Cooling	60.94% (exergy) 60.76% (electrical)	0.1232 £/kWh	Present study

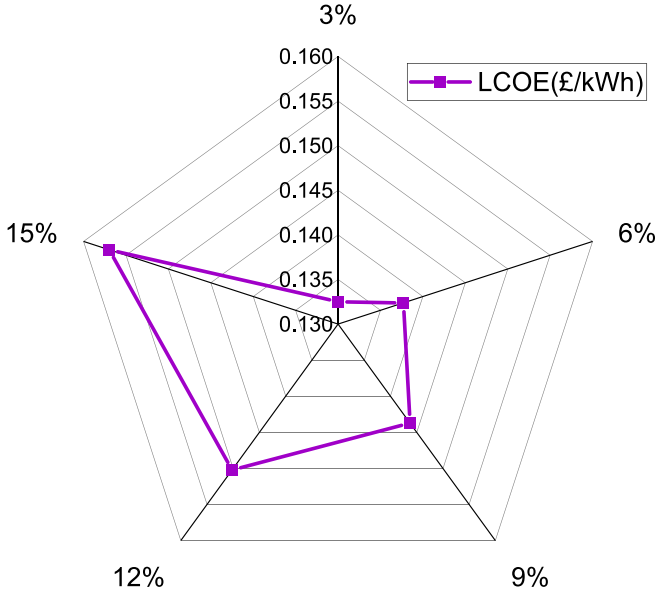

Fig. 13. Effect of interest rates on LCOE.

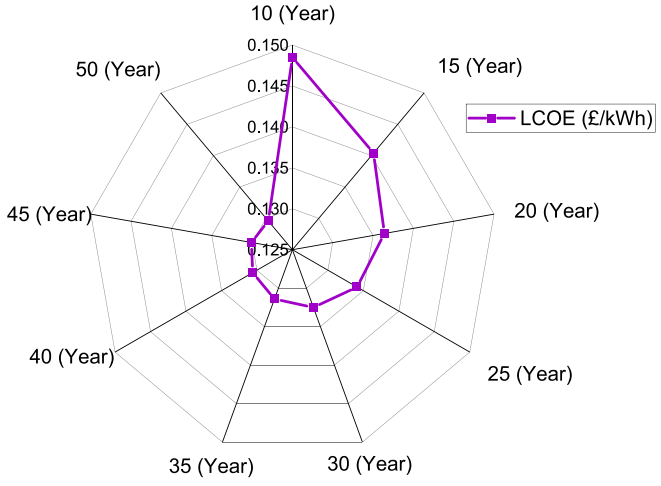

Fig. 14. Effect of operation years on LCOE.

chemical reactions, and mechanical wear. Additionally, SOFCs face challenges in accommodating fluctuating energy demands. To effectively address these challenges, further research will likely be necessary to develop an operational strategy for enhancing the system's adaptability.

CRediT authorship contribution statement

Dibyendu Roy: Writing – original draft, Software, Methodology, Conceptualization, Investigation, Data curation, Formal analysis. **Sumit Roy:** Writing – review & editing, Supervision, Methodology, Conceptualization. **Andrew Smallbone:** Writing – review & editing, Supervision, Resources, Project administration. **Anthony Paul Roskilly:** Writing – review & editing, Supervision, Project administration, Funding acquisition.

Declaration of Competing Interest

The authors declare that they have no known competing financial interests or personal relationships that could have appeared to influence the work reported in this paper.

Data availability

Data will be made available on request.

Acknowledgments

This research work was funded by the Engineering and Physical Science Research Council of UK (Grant numbers: EP/T022949/1).

References

[1] BEIS. Net Zero Strategy: Build Back Greener. 2021.
[2] Nature Editorials. Overhyping hydrogen as a fuel risks endangering net-zero goals. Nature 2022. https://doi.org/10.1038/d41586-022-03693-6.
[3] Minutillo M, Perna A, Di Trolio P, Di Micco S, Jannelli E. Techno-economics of novel refueling stations based on ammonia-to-hydrogen route and SOFC technology. Int J Hydrog Energy 2021;46:10059–71. https://doi.org/10.1016/j.ijhydene.2020.03.113.
[4] Cinti G, Frattini D, Jannelli E, Desideri U, Bidini G. Coupling solid oxide Electrolyser (SOE) and ammonia production plant. Appl Energy 2017;192:466–76. https://doi.org/10.1016/j.apenergy.2016.09.026.
[5] Afif A, Radenahmad N, Cheok Q, Shams S, Kim JH, Azad AK. Ammonia-fed fuel cells: a comprehensive review. Renew Sust Energ Rev 2016;60:822–35. https://doi.org/10.1016/j.rser.2016.01.120.
[6] Dolan RH, Anderson JE, Wallington TJ. Outlook for ammonia as a sustainable transportation fuel. Sustain Energy Fuels 2021;5:4830–41. https://doi.org/10.1039/d1se00979f.
[7] Miyazaki K, Muroyama H, Matsui T, Eguchi K. Impact of the ammonia decomposition reaction over an anode on direct ammonia-fueled protonic ceramic fuel cells. Sustain Energy Fuels 2020;4:5238–46. https://doi.org/10.1039/d0se00841a.
[8] Mojaver P, Khalilarya S, Chitsaz A. Performance assessment of a combined heat and power system: a novel integrated biomass gasification, solid oxide fuel cell and high-temperature sodium heat pipe system part I: thermodynamic analysis. Energy Convers Manag 2018;171:287–97. https://doi.org/10.1016/j.enconman.2018.05.096.
[9] Troskialina L, Arifin NA, Andarini RP, Muchtar A, Dhir A, Steinberger-Wilckens R. Effect of Sn loading variation on the electrochemical performance of dry internal reforming of biogas in solid oxide fuel cells. Int J Hydrog Energy 2023;48:1136–45. https://doi.org/10.1016/j.ijhydene.2022.10.020.
[10] Wang S, Liu X, Gu X, Huang X, Li Y. Analysis and multi-objective optimization of integrating a syngas-fed solid oxide fuel cell improved by a two-stage expander-

organic flash cycle using an ejector and a desalination cycle. Energy 2023:272. https://doi.org/10.1016/j.energy.2023.127095.
[11] Kim HR, Seo MH, Ahn JH, Kim TS. Thermodynamic design and analysis of SOFC/PEMFC hybrid systems with cascade effects: a perspective on complete carbon dioxide capture and high efficiency. Energy Rep 2023;9:2335–47. https://doi.org/10.1016/j.egyr.2023.01.048.
[12] Hu Y, Han C, Li W, Hu Q, Wu H, Luo Z. Experimental evaluation of methanol steam reforming reactor heated by catalyst combustion for kW-class SOFC. Int J Hydrog Energy 2023;48:4649–64. https://doi.org/10.1016/j.ijhydene.2022.10.274.
[13] Quach TQ, Giap VT, Keun Lee D, Pineda Israel T, Young Ahn K. High-efficiency ammonia-fed solid oxide fuel cell systems for distributed power generation. Appl Energy 2022;324:119718. https://doi.org/10.1016/j.apenergy.2022.119718.
[14] Sinha AA, Sanjay Ansari MZ, Shukla AK, Choudhary T. Comprehensive review on integration strategies and numerical modeling of fuel cell hybrid system for power & heat production. Int J Hydrog Energy 2023. https://doi.org/10.1016/j.ijhydene.2023.05.097.
[15] Al-Rashed AAAA, Alsarraf J, Alnaqi AA. A comparative investigation of syngas and biofuel power and hydrogen plant combining nanomaterial-supported solid oxide fuel cell with vanadium-chlorine thermochemical cycle. Fuel 2023;331:125910. https://doi.org/10.1016/j.fuel.2022.125910.
[16] Wang X, Duan L, Zheng N. Thermodynamic analysis of a novel tri-generation system integrated with a solar energy storage and solid oxide fuel cell – gas turbine. Appl Therm Eng 2023;219:119648. https://doi.org/10.1016/j.applthermaleng.2022.119648.
[17] Hou R, Zhang N, Gao W, Chen K, Liu Y. Thermodynamic, environmental, and exergoeconomic feasibility analyses and optimization of biomass gasifier-solid oxide fuel cell boosting a doable-flash binary geothermal cycle; a novel trigeneration plant. Energy 2023;265:126316. https://doi.org/10.1016/j.energy.2022.126316.
[18] Sinha AA, Saini G, Sanjay Shukla AK, Ansari MZ, Dwivedi G, et al. A novel comparison of energy-exergy, and sustainability analysis for biomass-fueled solid oxide fuel cell integrated gas turbine hybrid configuration. Energy Convers Manag 2023;283:116923. https://doi.org/10.1016/j.enconman.2023.116923.
[19] Fong KF, Lee CK. Performance investigation of a SOFC-primed micro-combined hybrid cooling and power system in hot and humid regions. Energy 2019;189:116298. https://doi.org/10.1016/j.energy.2019.116298.
[20] Cao Y, Elmasry Y, Singh PK, Alanazi A, Armghan A, Aly AA, et al. Thermo-environmental multi-aspect study and optimization of cascade waste heat recovery for a high-temperature fuel cell using an efficient trigeneration process. Appl Therm Eng 2023;221:119878. https://doi.org/10.1016/j.applthermaleng.2022.119878.
[21] Choudhary T, Sanjay.. Novel and optimal integration of SOFC-ICGT hybrid cycle: energy analysis and entropy generation minimization. Int J Hydrog Energy 2017;42:15597–612. https://doi.org/10.1016/j.ijhydene.2017.04.277.
[22] Kumar P, Choudhary T, Ansari MZ. Thermodynamic assessment of a novel SOFC and intercooled GT integration with ORC: energy and exergy analysis. Therm Sci Eng Prog 2022;34:101411. https://doi.org/10.1016/j.tsep.2022.101411.
[23] Sinha AA, Choudhary T, Ansari MZ, Sanjay.. Estimation of exergy-based sustainability index and performance evaluation of a novel intercooled hybrid gas turbine system. Int J Hydrog Energy 2023;48:8629–44. https://doi.org/10.1016/j.ijhydene.2022.10.260.
[24] Raj Singh U, Sai Kaushik A, Sekhar Bhogilla S. A novel renewable energy storage system based on reversible SOFC, hydrogen storage, Rankine cycle and absorption refrigeration system. Sustain Energy Technol Assess 2022;51:101978. https://doi.org/10.1016/j.seta.2022.101978.
[25] Xu Y, Luo X, Tu Z. 4E analysis of a SOFC-CCHP system with a LiBr absorption chiller. Energy Rep 2022;8:5284–95. https://doi.org/10.1016/j.egyr.2022.03.202.
[26] Zhang J, Cui P, Yang S, Zhou Y, Du W, Wang Y, et al. Thermodynamic analysis of SOFC–CCHP system based on municipal sludge plasma gasification with carbon capture. Appl Energy 2023;336:120822. https://doi.org/10.1016/j.apenergy.2023.120822.
[27] Mehrpooya M, Sadeghzadeh M, Rahimi A, Pouriman M. Technical performance analysis of a combined cooling heating and power (CCHP) system based on solid oxide fuel cell (SOFC) technology – a building application. Energy Convers Manag 2019;198:111767. https://doi.org/10.1016/j.enconman.2019.06.078.
[28] Zhao H, Lu R, Zhang T. Thermodynamic and economic performance study of SOFC combined cycle system using biomass and LNG coupled with CO2 recovery. Energy Convers Manag 2023;280:116817. https://doi.org/10.1016/j.enconman.2023.116817.
[29] Peng MYP, Chen C, Peng X, Marefati M. Energy and exergy analysis of a new combined concentrating solar collector, solid oxide fuel cell, and steam turbine CCHP system. Sustain Energy Technol Assess 2020;39:100713. https://doi.org/10.1016/j.seta.2020.100713.
[30] Akikur RK, Hajimolana RSKRUSA. Economic feasibility analysis of a solar energy and solid oxide fuel cell-based cogeneration system in Malaysia. Clean Technol environ. Policy 2016;18:669–87. https://doi.org/10.1007/s10098-015-1050-6.
[31] Cinti G, Discepoli G, Sisani E, Desideri U. SOFC operating with ammonia: stack test and system analysis. Int J Hydrog Energy 2016;41:13583–90. https://doi.org/10.1016/j.ijhydene.2016.06.070.
[32] Al-hamed KHM, Dincer I. A novel ammonia solid oxide fuel cell-based powering system with on-board hydrogen production for clean locomotives. Energy 2021;220:119771. https://doi.org/10.1016/j.energy.2021.119771.
[33] Selvam K, Komatsu Y, Sciazko A, Kaneko S, Shikazono N. Thermodynamic analysis of 100% system fuel utilization solid oxide fuel cell (SOFC) system fueled with ammonia. Energy Convers Manag 2021;249:114839. https://doi.org/10.1016/j.enconman.2021.114839.
[34] Du Y, Yang Z, Hou Y, Lou J, He G. Part-load performance prediction of a novel diluted ammonia-fueled solid oxide fuel cell and engine combined system with hydrogen regeneration via data-driven model. J Clean Prod 2023;395:136305. https://doi.org/10.1016/j.jclepro.2023.136305.
[35] United Nations. GOAL 7. Affordable and clean energy: ensure access to affordable, reliable, sustainable and modern energy for all. United Nations; 2023. https://sdgs.un.org/goals/goal7.
[36] Ranjbar F, Chitsaz A, Mahmoudi SMS, Khalilarya S, Rosen MA. Energy and exergy assessments of a novel trigeneration system based on a solid oxide fuel cell. Energy Convers Manag 2014;87:318–27. https://doi.org/10.1016/j.enconman.2014.07.014.
[37] Huang S, Yang C, Chen H, Zhou N, Tucker D. Coupling impacts of SOFC operating temperature and fuel utilization on system net efficiency in natural gas hybrid SOFC/GT system. Case Stud Therm Eng 2022;31:101868. https://doi.org/10.1016/j.csite.2022.101868.
[38] Roy D, Samanta S, Ghosh S. Techno-economic and environmental analyses of a biomass based system employing solid oxide fuel cell, externally fired gas turbine and organic Rankine cycle. J Clean Prod 2019;225:36–57. https://doi.org/10.1016/j.jclepro.2019.03.261.
[39] Van Veldhuizen BN, Van Biert L, Amladi A, Woudstra T, Visser K, Aravind PV. The effects of fuel type and cathode off-gas recirculation on combined heat and power generation of marine SOFC systems. Energy Convers Manag 2023;276:116498. https://doi.org/10.1016/j.enconman.2022.116498.
[40] Colonna P, Gabrielli S. Industrial trigeneration using ammonia-water absorption refrigeration systems (AAR). Appl Therm Eng 2003;23:381–96. https://doi.org/10.1016/S1359-4311(02)00212-0.
[41] Roy D, Samanta S. Development and multiobjective optimization of a novel trigeneration system based on biomass energy. Energy Convers Manag 2021;240:114248. https://doi.org/10.1016/j.enconman.2021.114248.
[42] Ghosh S, De S. Energy analysis of a cogeneration plant using coal gasification and solid oxide fuel cell. Energy 2006;31:345–63. https://doi.org/10.1016/j.energy.2005.01.011.
[43] Samanta S, Roy D, Roy S, Smallbone A, Roskilly AP. Techno-economic analysis of a fuel-cell driven integrated energy hub for decarbonising transportation. Renew Sust Energ Rev 2023;179:113278. https://doi.org/10.1016/j.rser.2023.113278.
[44] Wang Y, Yang J, Wang J, Guan W, Chi B, Jia L, et al. Low temperature ammonia decomposition catalyst and its application for direct ammonia-fueled solid oxide fuel cells. ECS Trans 2019;91:1611–9. https://doi.org/10.1149/09101.1611ecst.
[45] Mondal P, Ghosh S. Exergo-economic analysis of a 1-MW biomass-based combined cycle plant with externally fired gas turbine cycle and supercritical organic Rankine cycle. Clean Techn Environ Policy 2017;19:1475–86. https://doi.org/10.1007/s10098-017-1344-y.
[46] Khanmohammadi S, Atashkari K, Kouhikamali R. Exergoeconomic multi-objective optimization of an externally fired gas turbine integrated with a biomass gasifier. Appl Therm Eng 2015;91:848–59. https://doi.org/10.1016/j.applthermaleng.2015.08.080.
[47] Roy D, Samanta S, Ghosh S. Performance assessment of a biomass-fuelled distributed hybrid energy system integrating molten carbonate fuel cell, externally fired gas turbine and supercritical carbon dioxide cycle. Energy Convers Manag 2020;211:112740. https://doi.org/10.1016/j.enconman.2020.112740.
[48] Jackson CFK, GPHF. Ammonia to green hydrogen project:feasibility study. 2019.
[49] Patel M, Roy S, Roskilly AP, Smallbone A. The techno-economics potential of hydrogen interconnectors for electrical energy transmission and storage. J Clean Prod 2022;335:130045. https://doi.org/10.1016/j.jclepro.2021.130045.
[50] Curletti F, Gandiglio M, Lanzini A, Santarelli M, Maréchal F. Large size biogas-fed solid oxide fuel cell power plants with carbon dioxide management: technical and economic optimization. J Power Sources 2015;294:669–90. https://doi.org/10.1016/j.jpowsour.2015.06.091.
[51] Samanta S, Ghosh S. Techno-economic assessment of a repowering scheme for a coal fired power plant through upstream integration of SOFC and downstream integration of MCFC. Int J Greenh Gas Control 2017;64:234–45. https://doi.org/10.1016/j.ijggc.2017.07.020.
[52] Hosseinpour J, Chitsaz A, Liu L, Gao Y. Simulation of eco-friendly and affordable energy production via solid oxide fuel cell integrated with biomass gasification plant using various gasification agents. Renew Energy 2020;145:757–71. https://doi.org/10.1016/j.renene.2019.06.033.
[53] Bahari M, Entezari A, Esmaeilion F, Ahmadi A. Systematic analysis and multi-objective optimization of an integrated power and freshwater production cycle. Int J Hydrog Energy 2022;47:18831–56. https://doi.org/10.1016/j.ijhydene.2022.04.066.
[54] Hasanzadeh A, Chitsaz A, Mojaver P, Ghasemi A. Stand-alone gas turbine and hybrid MCFC and SOFC-gas turbine systems: comparative life cycle cost, environmental, and energy assessments. Energy Rep 2021;7:4659–80. https://doi.org/10.1016/j.egyr.2021.07.050.
[55] Keshavarzzadeh AH, Ahmadi P, Safaei MR. Assessment and optimization of an integrated energy system with electrolysis and fuel cells for electricity, cooling and hydrogen production using various optimization techniques. Int J Hydrog Energy 2019;44:21379–96. https://doi.org/10.1016/j.ijhydene.2019.06.127.
[56] Chitsaz A, Mehr AS, Mahmoudi SMS. Exergoeconomic analysis of a trigeneration system driven by a solid oxide fuel cell. Energy Convers Manag 2015;106:921–31. https://doi.org/10.1016/j.enconman.2015.10.009.
[57] Ebrahimi M, Keshavarz A, Jamali A. Energy and exergy analyses of a micro-steam CCHP cycle for a residential building. Energ Build 2012;45:202–10. https://doi.org/10.1016/j.enbuild.2011.11.009.
[58] Behnam P, Arefi A, Shafii MB. Exergetic and thermoeconomic analysis of a trigeneration system producing electricity, hot water, and fresh water driven by

low-temperature geothermal sources. Energy Convers Manag 2018;157:266–76. https://doi.org/10.1016/j.enconman.2017.12.014.

[59] Sornumpol R, Arpornwichanop A, Patcharavorachot Y. Performance analysis and optimization of a trigeneration process consisting of a proton-conducting solid oxide fuel cell and a LiBr absorption chiller. Int J Hydrog Energy 2023;48:6837–54. https://doi.org/10.1016/j.ijhydene.2022.05.169.

[60] Zang G, Zhang J, Ratner A, Shi Y. Techno-economic analysis of a cooling, heating, and electricity trigeneration system based on downdraft fixed bed wood and tire gasification: case study of a campus office building. Sustain Energy Technol Assess 2023;55:102939. https://doi.org/10.1016/j.seta.2022.102939.